Mechanical Systems and Signal Processing 105 (2018) 1–15

Contents lists available at ScienceDirect

Mechanical Systems and Signal Processing

journal homepage: www.elsevier.com/locate/ymssp

A comparison of linear approaches to filter out environmental effects in structural health monitoring

A. Deraemaeker [a,*], K. Worden [b]

[a] Université Libre de Bruxelles (ULB) – BATir, 50 av Franklin Roosevelt, CP 194/02, 1050 Brussels, Belgium
[b] Dynamics Research Group, Department of Mechanical Engineering, University of Sheffield, Mappin Street, Sheffield S1 3JD, UK

ARTICLE INFO

Article history:
Received 7 September 2017
Received in revised form 22 November 2017
Accepted 30 November 2017
Available online 22 December 2017

Keywords:
Structural Health Monitoring (SHM)
Environmental effects
Mahalanobis squared-distance
Principal Component Analysis (PCA)
Factor analysis

ABSTRACT

This paper discusses the possibility of using the Mahalanobis squared-distance to perform robust novelty detection in the presence of important environmental variability in a multivariate feature vector. By performing an eigenvalue decomposition of the covariance matrix used to compute that distance, it is shown that the Mahalanobis squared-distance can be written as the sum of independent terms which result from a transformation from the feature vector space to a space of independent variables. In general, especially when the size of the features vector is large, there are dominant eigenvalues and eigenvectors associated with the covariance matrix, so that a set of principal components can be defined. Because the associated eigenvalues are high, their contribution to the Mahalanobis squared-distance is low, while the contribution of the other components is high due to the low value of the associated eigenvalues. This analysis shows that the Mahalanobis distance naturally filters out the variability in the training data. This property can be used to remove the effect of the environment in damage detection, in much the same way as two other established techniques, principal component analysis and factor analysis. The three techniques are compared here using real experimental data from a wooden bridge for which the feature vector consists in eigenfrequencies and modeshapes collected under changing environmental conditions, as well as damaged conditions simulated with an added mass. The results confirm the similarity between the three techniques and the ability to filter out environmental effects, while keeping a high sensitivity to structural changes. The results also show that even after filtering out the environmental effects, the normality assumption cannot be made for the residual feature vector. An alternative is demonstrated here based on extreme value statistics which results in a much better threshold which avoids false positives in the training data, while allowing detection of all damaged cases.

1. Introduction

Vibration-based Structural Health Monitoring (SHM) techniques have been around for many years and are still today an active topic of research. Despite this fact, very few industrial applications exist. Two major trends coexist in the field: model-based and data-based techniques. Model-based techniques are often sophisticated and require a high degree of engineering

* Corresponding author.
E-mail address: aderaema@ulb.ac.be (A. Deraemaeker).

https://doi.org/10.1016/j.ymssp.2017.11.045
0888-3270/

knowledge and heavy hardware and software resources; they have however more potential to cover all levels of SHM, from damage detection to damage prognosis. On the other hand, data-based techniques are appealing as they require less engineering knowledge as well as limited hardware and software resources. From that point of view, they are ideal candidates for industrial applications. These methods are however generally limited to the lowest levels of SHM: damage detection and in some cases, damage localisation or classification and severity if training data are available [1].

Data-based damage detection techniques consist in detecting a deviation from the normal condition based only on undamaged-state data measured on the structure or system to be monitored. This paper focuses on the use of vibration data collected at regular time intervals. A further step consists in feature extraction, i.e. transforming these time series data into meaningful information, called features (the most common being the mode shapes and eigenfrequencies). The stochastic nature of the excitation and the unavoidable added noise on the measured data results in features having a stochastic nature. This fact being recognised, it is natural to turn to statistical methods to monitor them and detect any significant deviation from the normal condition.

The three basic elements of data-based damage detection are therefore (i) a permanent sensor network system, (ii) an automated procedure for real-time or periodic feature extraction, and (iii) a robust novelty detector [2]. The first element has received much attention in the last decade and the enormous advances in sensors and instrumentation make it possible today to deploy very large sensor networks on structures and gather the measured data in central recording units at high sampling rates. The second element is still today a challenge, and for the most widely-used features (eigenfrequencies and mode shapes) is an active topic of research [3,4]. An alternative is to look at other features which can easily be extracted automatically from the time domain data. Several efforts have been made in that direction, such as the use of residuals based on Hankel matrices [5], or peak indicators in the frequency output of modal filters [3]. For the third element, different approaches have been borrowed from statistics and machine learning, the most commonly used being control charts [6], outlier analysis using the Mahalanobis squared-distance [7] (which is similar to Hoteling T^2 control charts for individual measurements) or hypothesis testing [5].

This paper focuses on the third element of the data-based damage detection system in the presence of confounding effects due to environmental and operational variability. Important variability of the dynamic properties of structures under ambient vibrations has been identified in a number of studies [8–11]. These studies highlight the fact that variations in the dynamic characteristics due to confounding effects (temperature, humidity, traffic, wind) can be of the same order of magnitude as, or greater than, the variations due to damage, which hinders detection of the onset of damage. In the context of data-based damage detection, which is the focus of this paper, several methods have been proposed in order to filter out these effects. The simplest methods are based on the identification of the linear subspace to which the environmental and operational conditions belong, in order to remove their effect on the monitored features. Such methods are well suited when the dimension of the feature vector is large enough to be able to find a linear subspace to which the confounding effects belong. When such is not the case, non-linear methods which consist in identifying a non-linear manifold instead of a linear subspace can be used [12–14]. These techniques are however much more complex and computationally costly. The present paper has two aims: (i) to show that the Mahalanobis squared-distance can be used to filter out confounding effects in a very similar way to the linear techniques, and (ii) to demonstrate the link between the aforementioned technique and the two most commonly used linear techniques to filter confounding effects: principal component analysis [15] and factor analysis [16].

This paper is organised as follows: the second section details the mathematical foundations of the methodology proposed to filter out confounding effects based on the Mahalanobis squared-distance. The third section presents briefly the two most commonly-used linear techniques for filtering out confounding effects: principal component analysis and factor analysis, and shows the link with the method proposed in Section 2. In the fourth section, the three techniques are applied on data acquired from a wooden bridge under changing environmental conditions. The results clearly demonstrate the strong similarities between the three techniques.

2. Multivariate novelty detection under changing environmental conditions

2.1. The Mahalanobis squared-distance

Consider a set of N feature vectors $\{y_i\}$ $(i = 1 \dots N)$ of dimension n, representing N samples of the 'healthy state' of a structure, of which the mean vector $\{\overline{y}\}$ of size $n \times 1$ and the covariance matrix $[C]$ of size $n \times n$ can be estimated as follows,

$$\{\overline{y}\} = \frac{1}{N}\sum_{i=1}^{N}\{y_i\} \tag{1}$$

$$[C] = \frac{1}{N-1}\sum_{i=1}^{N}(\{y_i\} - \{\overline{y}\})(\{y_i\} - \{\overline{y}\})^T \tag{2}$$

The multivariate feature vectors correspond to the features extracted from the vibration measurements such as a set of eigenfrequencies, modeshapes, FRF or transmissibility functions at given frequencies, etc. (Throughout this paper, curved braces denote vectors, and square braces denote matrices).

The principle of outlier analysis [7] is, for each sample of the multivariate feature vector $\{y_\zeta\}$, to compute the Mahalanobis squared-distance [17] given by,

$$D_\zeta^2 = (\{y_\zeta\} - \{\overline{y}\})^T [C]^{-1} (\{y_\zeta\} - \{\overline{y}\}) \tag{3}$$

Computing D_ζ for all the data in the training set used to compute $[C]$, it is possible to set a threshold. If a new sample $\{y_\zeta\}$ of the feature vector results in a value of D_ζ above this threshold, it will be considered as an outlier. Outlier analysis can be *inclusive* in the case that the damaged data is included for the computation of the mean vector and covariance matrix, or *exclusive* in the case that only the undamaged data are used.

Outlier analysis using the Mahalanobis squared-distance has been used in various application fields such as tool condition monitoring [18,19], monitoring of cracking in concrete [20], monitoring of railroad tracks [21] or disease diagnosis [22]. This distance is also used for multivariate data classification in the Mahalanobis-Taguchi strategy (MTS) [23–27].

2.2. Spectral decomposition

In most cases, the features in the data vector are not statistically independent, so that the covariance matrix is not diagonal. It is however possible to perform a transformation of the feature vector in order to diagonalise the covariance matrix. This is done by computing the eigenvectors $\{U_i\}$ and eigenvalues σ_i^2 of $[C]$,

$$[C]\{U_i\} = \sigma_i^2 \{U_i\} \tag{4}$$

The orthogonality properties are given by,

$$[U]^T [C][U] = [S] \tag{5}$$

$$[U]^T [U] = [I] \tag{6}$$

where $[U]$ is the matrix whose columns contain all the eigenvectors, $[S]$ is a diagonal matrix containing the eigenvalues σ_i^2 in descending order of magnitude on the diagonal, and $[I]$ is the identity matrix. The spectral decomposition of the covariance matrix is given by,

$$[C] = [U][S][U]^T \tag{7}$$

and the spectral decomposition of the inverse of the covariance matrix by,

$$[C]^{-1} = [U][S]^{-1}[U]^T \tag{8}$$

Assuming now the following transformation,

$$\{\eta_i\} = [U]^T \{y_i\} \tag{9}$$

The mean and covariance matrix estimated from the N transformed samples η_i $(i = 1 \ldots N)$ are given by,

$$\{\overline{\eta}\} = \frac{1}{N} \sum_{i=1}^{N} \{\eta_i\} = [U]^T \{\overline{y}\} \tag{10}$$

$$[C]_\eta = \frac{1}{N-1} \sum_{i=1}^{N} (\{\eta_i\} - \{\overline{\eta}\})(\{\eta_i\} - \{\overline{\eta}\})^T \tag{11}$$

$$= [U]^T \frac{1}{N-1} \sum_{i=1}^{N} (\{y_i\} - \{\overline{y}\})(\{y_i\} - \{\overline{y}\})^T [U] \tag{12}$$

$$= [U]^T [C][U] \tag{13}$$

and by using the orthogonality condition, one sees directly that the covariance matrix of $\{\eta\}$ is diagonal and that the standard deviation of each component η_i is given by σ_i, via,

$$[U]^T [C][U] = [S] \tag{14}$$

Using the inverse transformation,

$$\{y_i\} = [U]\{\eta_i\} \tag{15}$$

the Mahalanobis squared-distance reduces to,

$$D_\zeta^2 = \sum_{i=1}^{n} \frac{1}{\sigma_i^2} (\eta_{\zeta i} - \overline{\eta}_i)^2 \tag{16}$$

This shows that the Mahalanobis squared-distance can be decomposed into a sum of independent contributions from each component of the transformed variables $\eta_{\zeta i} = \{U_i\}^T \{y_\zeta\}$. The contributions are weighted by the inverse of the associated eigenvalues σ_i^2, which can be interpreted as the variances of the new, transformed variables. If the variance is large, the contribution to the distance is small.

2.3. Filtering of the environmental effects

In many cases, when the number of features is large enough, the total variability in the feature vector extracted from the healthy condition can be explained by a smaller number of transformed features, usually called the principal component scores. Strictly speaking, this occurs when some of the eigenvalues of $[C]$ are equal to zero. The associated eigenvectors form the null-space (or kernel) of the training data. In practice, due to the noise and numerical precision issues, the eigenvalues are not strictly equal to zero, but a significant drop in the eigenvalues can be observed and can be used to define the number of principal components which account for most of the variability. An effective null-space is defined by putting a threshold on the singular values, assuming that the singular values below this threshold are only non-zero due to the noise in the training data. In the following, the effective null-space or kernel will simply be called the 'null-space' or 'kernel'. A practical way to determine the number p of vectors in the principal subspace is to define the following indicator,

$$I = \frac{\sum_{i=1}^{p} \sigma_i^2}{\sum_{i=1}^{n} \sigma_i^2} \tag{17}$$

and to determine p as the lowest integer such that $I > e(\%)$, where e is a threshold value (i.e. 99.9%). The meaning of this threshold is as follows: p principal components are needed in order to explain $e\%$ of the variance in the observed data. Assume that these p principal components have been identified. For a new sample of the feature vector $\{y_\zeta\}$, the Mahalanobis squared-distance can be decomposed into two parts,

$$D_\zeta^2 = \sum_{i=1}^{p} \frac{1}{\sigma_i^2} (\eta_{\zeta i} - \overline{\eta}_i)^2 + \sum_{i=p+1}^{n} \frac{1}{\sigma_i^2} (\eta_{\zeta i} - \overline{\eta}_i)^2 = D_{1\zeta}^2 + D_{2\zeta}^2 \tag{18}$$

where $D_{1\zeta}^2$ is the Mahalanobis squared-distance of $\{y_\zeta\}$ projected on the principal components, and $D_{2\zeta}^2$ is the Mahalanobis squared-distance of $\{y_\zeta\}$ projected on to the null-space of the principal components.

If one now assumes that very large variability exists in the feature vector extracted from the healthy condition due to environmental effects, if this variability is more important than other sources such as noise, it will belong to the set of the first p principal components. Because the Mahalanobis squared-distance scales each independent component with respect to the inverse of its variance, the distance will have a very low sensitivity to the environmental changes. By including the feature vector measured in all possible environmental conditions in the computation of the covariance matrix, the Mahalanobis squared-distance is made insensitive to the environmental conditions. This idea will be demonstrated in Section 4 on a laboratory experiment.

3. Principal component analysis and factor analysis

The way principal component analysis can be used to filter out confounding effects is to project the feature vector onto the subspace of the minor components, when the major components have been identified on data containing variability to confounding effects [28,29]. If the Mahalanobis squared-distance is subsequently used to perform outlier analysis, it reduces to computing,

$$D_\zeta^2 = \sum_{i=p+1}^{n} \frac{1}{\sigma_i^2} (\eta_{\zeta i} - \overline{\eta}_i)^2 = D_{2\zeta}^2 \tag{19}$$

which is equivalent to considering that $\sigma_i = \infty$ for $i \leqslant p$. One can easily see that if there is a clear drop in the σ_i values, computing the full Mahalanobis squared-distance is equivalent to computing the Mahalanobis squared-distance of the feature vector projected on to the subspace of minor components.

This is illustrated with the following example: in Fig. 1, the feature vectors in two dimensions have been built from two normal distributions with $\sigma_1 = 3$ and $\sigma_2 = 1$ and using a rotation angle of $\pi/3$. Equidistant points from the mean lie on an ellipse which is rotated at an angle $\pi/3$ with respect to the features axis. As σ_1 and σ_2 are of the same order of magnitude, there is no possibility to clearly define the linear subspace to which the confounding effects belongs.

In Fig. 2, consider now the same case but with $\sigma_2 = 0.1$. One can see clearly that the feature vectors almost lie on a line, which is a subspace of the feature vector space. The Mahalanobis squared-distance can be decomposed into two independent terms. The first term corresponds to the projection of the feature vector in the direction of the line (direction with large σ_i). This term is only sensitive to a change of the feature vector in the principal direction. Looking only at this contribution corresponds to projecting the feature vector on the first principal component. One notes however, that the contribution to the Mahalanobis squared-distance will be weak because the distance is weighted by $1/\sigma_1^2$ where σ_1 is large. The second term

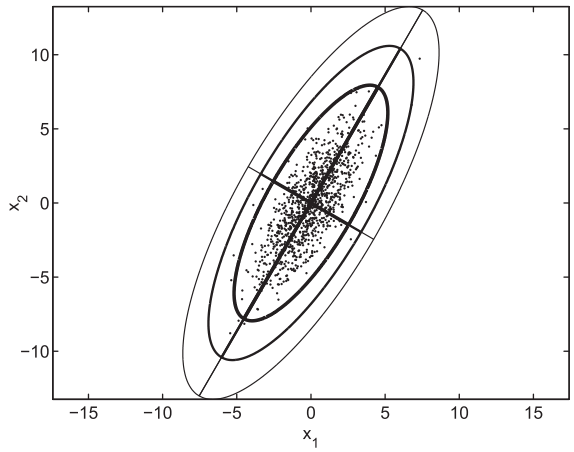

Fig. 1. Equidistant points in the sense of the Mahalanobis squared-distance. x_1 and x_2 built from two normal distribution with $\sigma_1 = 3$ and $\sigma_2 = 1$ using a rotation angle of $\pi/3$.

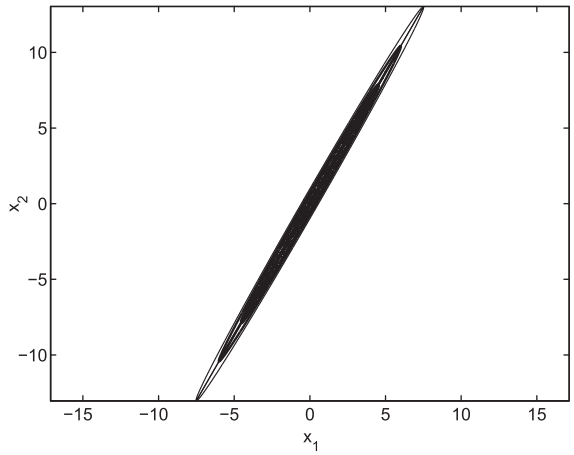

Fig. 2. Equidistant points in the sense of the Mahalanobis squared-distance. x_1 and x_2 built from two normal distribution with $\sigma_1 = 3$ and $\sigma_2 = 0.1$ using a rotation angle of $\pi/3$.

corresponds to the projection of the feature vector on the direction perpendicular to the line (direction with small σ_i). This term is only sensitive to a change of the feature vector in the minor direction (in opposition with the principal direction). Looking only at this contribution corresponds to projecting the feature vector on the direction orthogonal to the principal component. The contribution to the Mahalanobis squared-distance will be very strong because it is weighted by $1/\sigma_2^2$ where σ_2 is very low.

The procedure to identify the linear subspace and to project the data on to the orthogonal subspace is slightly different in factor analysis [16]. In order to show this, the theory behind it and the link with principal component analysis is briefly recalled in the following.

Assume, as previously, that all the features are arranged in a vector $\{y\}$ and one can write,

$$\{y\} = f(T, h, \ldots) + g(\{v\}) \tag{20}$$

where $\{v\}$ is the vector of variables independent of the environment (i.e. damage, noise, ...), and $(T, h, \ldots)$ are the confounding effects (i.e. Temperature, humidity, ...). In general, the function f is very difficult to identify, the general form being dependent on the structure considered and the type of features extracted. This general mapping function f can be decomposed into two different mappings as shown in Fig. 3. The environmental factors $(T, h \ldots)$ are transformed into a vector of *unobservable factors* $\{\xi\}$, by means of a non-linear mapping $\mathcal{M}$,

$$f(T, h, \ldots) = [\Lambda](\mathcal{M}(T, h, \ldots)) \tag{21}$$

The terminology *unobservable factors* is used in factor analysis [30]. This non-linear mapping is generally unknown and there is no need to identify it in the present application. The *unobservable factors* $\{\xi\}$ are assumed to be statistically uncor-

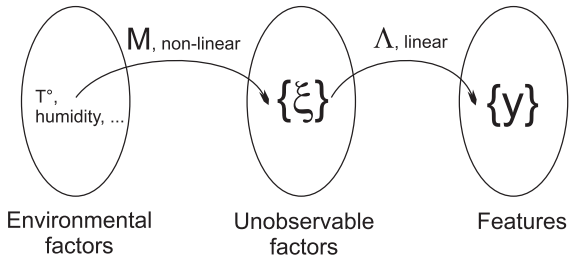

Fig. 3. Function f relating the dynamical features with the environmental variables is decomposed into a non-linear mapping $\mathcal{M}$ and a linear mapping Λ, introducing statistically independent *unobservable factors* $\{\xi\}$.

related variables with unit standard deviation. In linear factor analysis, a linear mapping Λ is used between the *unobservable factors* and the features. Eq. (20) becomes,

$$\{y\} = [\Lambda]\{\xi\} + g(\{v\}) \tag{22}$$

If the number of *unobservable factors* is equal to the number of features, $[\Lambda]$ is a rotation matrix resulting in an orthogonalisation of the feature vector $\{y\}$. In this case $g(\{v\}) = 0$ and the environment cannot be distinguished from the other variables in $\{v\}$. In order to remove the effects of the environment and keep information about damage, the dimension of $\{\xi\}$ needs to be smaller than the number of features. One important parameter to be determined in the method is therefore the number of *unobservable factors*. This issue is very similar to the one of finding the number of principal components discussed earlier.

In order to identify the linear mapping $[\Lambda]$ between the *unobservable factors* and the features, it is necessary to measure the feature vector under changing environmental conditions, while the influence of other factors $\{\varepsilon\}$ is small.

$$\{\varepsilon\} = g(\{v\}) \ll [\Lambda]\{\xi\} \tag{23}$$

This requires the extraction of features from the undamaged structure during a period of time in which all of the environmental effects to be removed manifest themselves (i.e. monitoring a bridge after construction during a one year period of time). In factor analysis, $\{\varepsilon\}$ is the vector of *unique factors* which are assumed to be uncorrelated and independent from the *unobservable factors*. Assume that N samples $\{y_i\}$ $(i = 1..N)$ of the feature vector $\{y\}$ have been measured during a certain period of time. The covariance matrix of the features is $[C]$ as defined previously. Using the factor model (Fig. 4), each sample of the feature vector is written in the form,

$$\{y_i\} = [\Lambda]\{\xi_i\} + \{\varepsilon_i\} \tag{24}$$

Due to the statistical hypothesis on $\{\xi\}$ and $\{\varepsilon\}$, the covariance matrix can be written,

$$[C] = [\Lambda][\Lambda]^T + [\Psi] \tag{25}$$

where $[\Psi]$ is the covariance matrix of $\{\varepsilon\}$, assumed to be diagonal (*unique factors* are uncorrelated). The identification of the factor model consists in splitting the covariance matrix of measured features into the contribution of the environment and the residual part. This is possible because of the assumption that $||\{\varepsilon\}|| \ll ||[\Lambda]\{\xi\}||$ (in some appropriate norm). Several

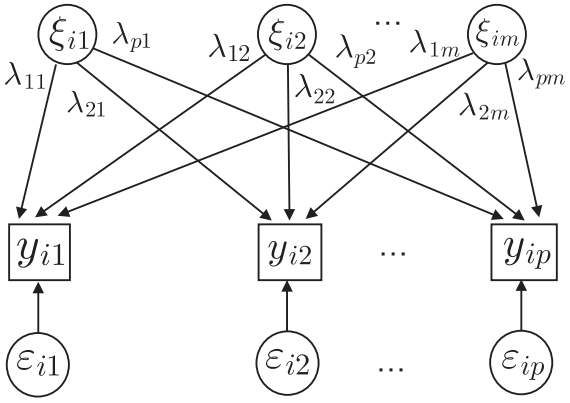

Fig. 4. Orthogonal factor model.

methods exist to identify the factor model. The method used in [16] and detailed in [30] is presented. The method is iterative. It starts with the definition of the *communalities* which are the diagonal elements of,

$$[C]^* = [\Lambda][\Lambda]^T \tag{26}$$

The iterations are carried out on $[C]^*$, starting with $[C]^* = [C]$:

- Compute the eigenvalues σ_i^2 and eigenvectors U_i of matrix $[C]^*$
- Determine the p eigenvectors needed to represent $e\%$ of the variance in the data and take

$$[\Lambda] = \left[\frac{1}{\sigma_1}U_1 \frac{1}{\sigma_2}U_2 \dots \frac{1}{\sigma_p}U_p\right] \tag{27}$$

- Compute the new communalities which are the diagonal elements of $[\Lambda][\Lambda]^T$ and replace the diagonal elements of $[C]^*$ with the new communalities.
- Iterate until the values of the communalities have converged.

The output of the algorithm is the matrix $[\Lambda]$. The diagonal matrix $[\Psi]$ can be computed easily from,

$$[\Psi] = [C] - [\Lambda][\Lambda]^T \tag{28}$$

From the algorithm above, the link with PCA is straightforward. It corresponds to the first iteration of the method in which the first p eigenvectors of $[C]$ are computed. After this first iteration, the subspace spanned by the vectors of $[\Lambda]$ is the subspace of the principal components as defined earlier. Note however that in PCA, the vectors are usually not normalised ($1/\sigma_i$ multiplying factor used in FA). The resulting subspaces are however identical. At this point, the following remarks should be made:

- As the influence of the unique factors is very small if e is high enough (i.e. $e = 99.9\%$ is a common choice), the algorithm for FA converges very fast and there is only a very slight difference between the first estimate of $[\Lambda]$ and the converged value. The subspaces identified with PCA and FA are therefore very close.
- It is not obvious that the matrix $[\Psi]$ should be a diagonal matrix in SHM applications. Most of the features extracted for SHM contain some noise which is not added directly and independently on each feature, but results from the noise in the data acquisition chain which has been transformed in the feature extraction process, causing very likely correlations between the noise on the different features (see for example the study for mode shapes in [31]).

Once the matrix $[\Lambda]$ has been identified, the removal of the environmental effects consists in determining the best approximation of the feature vector $\{y\}$,

$$\{\hat{y}\} = [\Lambda]\left\{\hat{\xi}\right\} \tag{29}$$

and in removing it from the feature vector in order to build a residual,

$$\{\varepsilon\} = \{y\} - [\Lambda]\left\{\hat{\xi}\right\} \tag{30}$$

There are several choices in order to build the best approximations, but previous studies have shown that all of them lead to very similar results. The simplest approximation is based on ordinary least squares giving the following estimate,

$$\left\{\hat{\xi}\right\} = \left([\Lambda]^T[\Lambda]\right)^{-1}[\Lambda]^T\{y\} \tag{31}$$

which reduces to,

$$\left\{\hat{\xi}\right\} = [S^*]^{-1}[\Lambda]^T\{y\} \tag{32}$$

where $[\Lambda]^T[\Lambda] = [S^*]$ is a diagonal matrix with the eigenvalues $\sigma_i^2,\ i = 1..p$ on the diagonal. This solution is the one that minimises the L_2-norm of the error given by,

$$\|\{y\} - [\Lambda]\left\{\hat{\xi}\right\}\|^2 = \left(\{y\} - [\Lambda]\left\{\hat{\xi}\right\}\right)^T\left(\{y\} - [\Lambda]\left\{\hat{\xi}\right\}\right) \tag{33}$$

An alternative to this approach is to use generalised least-squares where the norm contains a weighting matrix $[W]$, such that,

$$\|\{y\} - [\Lambda]\left\{\hat{\xi}\right\}\|_W^2 = \left(\{y\} - [\Lambda]\left\{\hat{\xi}\right\}\right)^T[W]\left(\{y\} - [\Lambda]\left\{\hat{\xi}\right\}\right) \tag{34}$$

The minimum of this norm is given by:

$$\left\{\hat{\xi}\right\} = \left([\Lambda]^T[W][\Lambda]\right)^{-1}[\Lambda]^T[W]\{y\} = [\Lambda]^T\{y\} \tag{35}$$

A typical choice for the weighting matrix is $[W] = [C]^{-1}$. Although there are some sound statistical reasons for that, a physical understanding is the fact that less weight is put on the data with the highest variance in the calculation of the estimate. Note that in the particular case studied here, assuming that $\|[\Psi]\| \ll \|[\Lambda]^T[\Lambda]\|$ (again, in some appropriate norm), the inverse of the covariance matrix can be approximated by,

$$[C]^{-1} \simeq [\Lambda][S^*]^{-2}[\Lambda]^T \tag{36}$$

and Eq. (35) reduces to,

$$\left\{\hat{\xi}\right\} = [S^*]^{-1}[\Lambda]^T\{y\} \tag{37}$$

which is identical to Eq. (32). Other alternatives can be based on Bartlett's and Thomson's factor score which have been found to give very similar results [32]. In this study, Eq. (32) will be used. The residual can be written,

$$\{\varepsilon\} = \{y\} - [\Lambda][S^*]^{-1}[\Lambda]^T\{y\} = \left([I] - [\Lambda][S^*]^{-1}[\Lambda]^T\right)\{y\} \tag{38}$$

It is equal to the projection of the feature vector in the null-space of the subspace spanned by the vectors of $[\Lambda]$, which, as discussed earlier, is the subspace of the principal components if a single iteration is used in FA.

The above developments clearly show the link between PCA and FA, and how these two methods can be related to the use of the Mahalanobis squared-distance proposed in Section 2. This is further illustrated in the next section where the three methods are applied to data from a laboratory experiment.

4. Application: Wooden bridge

Consider the wooden bridge shown in Fig. 5, equipped with a monitoring system, previously developed and investigated in [33]. The total mass of the bridge is 36 kg. A random excitation was applied using an electrodynamic shaker and output-only acceleration measurements were collected at 15 different locations. Mode shapes and eigenfrequencies were extracted from the measurements using output-only stochastic subspace identification. The monitoring was performed over several days during which modal properties varied significantly due to temperature and humidity changes. Out of the 16 modes identified, only modes 6–8, 10 and 12–16 are used in this study. The first five modes correspond to low frequency modes related to rigid body motion of the bridge involving strain in the supports only, while modes 9 and 11 were not found consistently in all datasets, which is the reason for discarding them. In total, 1880 measurements were performed on the undamaged structure under changing environmental conditions. Samples 1881 to 1985 then correspond to the incremental addition of a local mass of 23.5 g, 47 g, 70.5 g, 123.2 g and 193.7 g at samples 1881, 1901, 1924, 1946 and 1966 respectively, which are considered as the damaged conditions here. Samples 1986 to 2008 correspond to measurements on the bridge where all masses have been removed (return to undamaged condition).

Fig. 6 shows the variation of natural frequency six with respect to the sample number. It is clear that environmental conditions are responsible for frequency changes of an order of magnitude larger than the damage (simulated here with an added mass).

The feature vector is made of nine natural frequencies and nine mode shapes measured at 15 locations. The mode shapes are complex and normalised with respect to the first component, so that 14×2 values are used in the feature vector for each

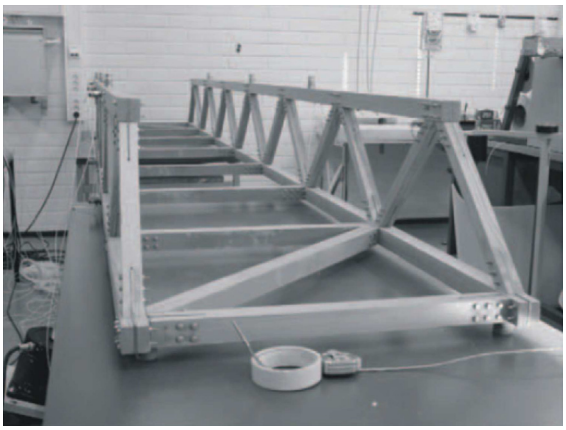

Fig. 5. Wooden bridge equipped with a monitoring system [33].

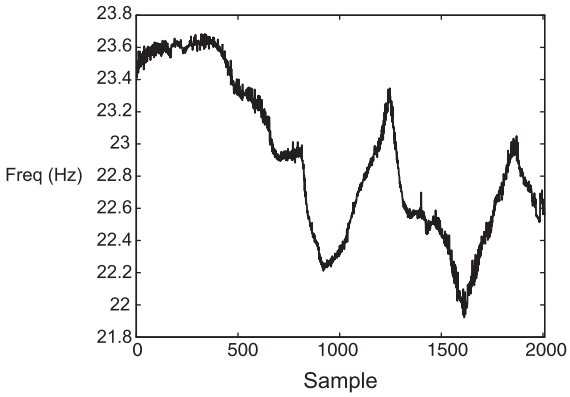

Fig. 6. Evolution of the 6th natural frequency of the bridge with respect to sample number.

mode shape, resulting in a feature vector y of dimension 261 (9 frequencies + $14 \times 2 \times 9$ mode shape components). Each component of the feature vector is then standardised with respect to the mean and standard deviations computed on the training data.

4.1. Filtering of the environmental effects using the Mahalanobis squared-distance

Fig. 7 shows the evolution of the Mahalanobis squared-distance computed for each of the 2008 samples when considering the first 300, 1000 and 1880 samples for the computation of the covariance matrix (training data). It is clear from the results that the Mahalanobis squared-distance acts as a filter for the environmental variations which have been used for the computation of the covariance matrix. When using the first 300 and 1000 samples, the value of the Mahalanobis squared-distance for some of the healthy samples (not used for the computation of the covariance matrix) is of the same order of magnitude as for the samples with the structural change. In this case, the novelty detection is hindered by the environmental changes. When including all the variability from the environment in the computation of the covariance matrix, the Mahalanobis squared-distance has a low sensitivity to environmental changes and is very sensitive to structural changes.

4.2. Comparison with principal component analysis and factor analysis

The residual of the feature vector is computed for each sample using either PCA or FA. Fig. 8a shows the result when only the first iteration is used in FA and the first 1880 samples are used as training data, confirming that it is identical to PCA. Note that the same number of principal components/unobservable factors has been used with the two methods ($e = 99.9\%$ was used to find $p = 81$). Fig. 8b compares the results of PCA with FA after convergence of the iterative process. The differences are very minor and difficult to detect.

In Fig. 9, the results of FA and PCA are compared to the results previously obtained where no pre-processing of the feature vector is performed (raw data). Samples (1–1880) are used for the computation of the covariance matrix in all cases. As expected, PCA and FA do not bring a major improvement in the damage detection.

4.3. Threshold setting and damage detection using the Mahalanobis squared-distance

In order to assess the possibility of using the Mahalanobis squared-distance to perform damage detection under changing environmental conditions, 80% of the undamaged samples under changing environmental conditions were used to compute the mean vector and the covariance matrix. The training samples were picked randomly amongst the 1880 samples, resulting in 1504 training feature vectors of size 261. The remaining 376 samples were used as testing set, together with samples 1986–2008 (undamaged after removal of the masses).

In order to detect damage, it is necessary to set a threshold above which the condition of the system will be considered as abnormal. This value is dependent on both the number of observations and the dimension of the feature vector. The value also depends upon whether an inclusive or exclusive threshold is calculated. Another important parameter is the confidence level α which is set here to 0.001 (this sets the limit so that it is normal to have statistically 1 out of 1000 samples above the threshold).

The first approach to set the threshold makes the assumption that the residual vector is normally distributed. A Monte-Carlo simulation is used, summarised as follows [7]:

- Construct a (261×1504) matrix with each element being a randomly generated number from a zero mean and unit standard deviation normal distribution.

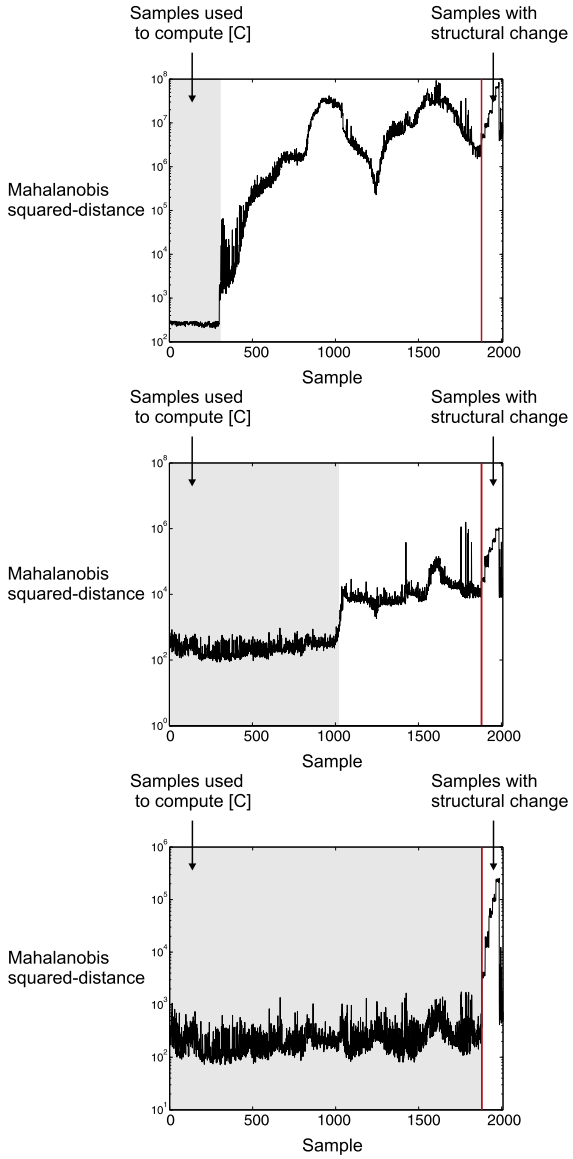

Fig. 7. Evolution of the Mahalanobis squared-distance with respect to sample number when the covariance matrix is computed with 300, 1000 and 1880 (all) healthy samples.

- Calculate the Mahalanobis squared-distance for all the observations, and store the largest value.
- Repeat the process 1000 times and store the largest value of the Mahalanobis squared-distance for each process.

The inclusive threshold T_{inc} is the value of the largest of the 1000 values stored, and the exclusive threshold can be computed from,

$$T_{exc} = \frac{(n-1)(n+1)^2 T_{inc}}{n(n^2-(n+1)T_{inc})} \tag{39}$$

where n is the number of training samples ($n = 1504$). The result is shown in Fig. 10. It is clear that the threshold is too low, as there are numerous false positives both in the training and the testing set. This is due to the fact that the normality assumption is not correct.

An alternative is to use extreme value statistics to compute the threshold. The methodology is described in [34,35]. The first steps consists in fitting a parametric model to the right tail of the empirical cumulative density function (CDF) of the training data. It is shown in [36] that when looking at the distribution of maxima, there are only three possible distributions: the Gumbel, Frechet and Weibull distributions. The approach consists in fitting the parameters of these three distributions

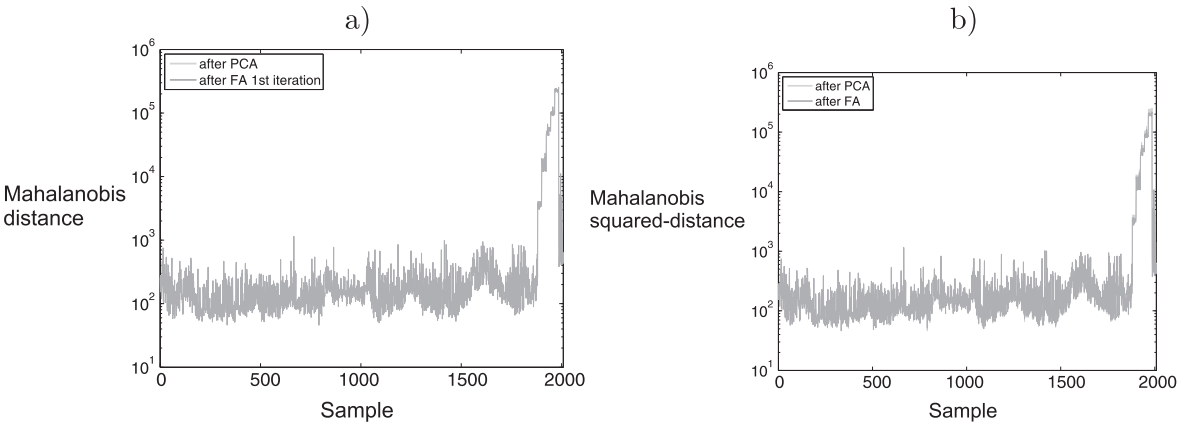

Fig. 8. Comparison of the Mahalanobis squared-distance computed after PCA and (a) FA using a single iteration and (b) FA after convergence (the first 1880 samples are used as training data).

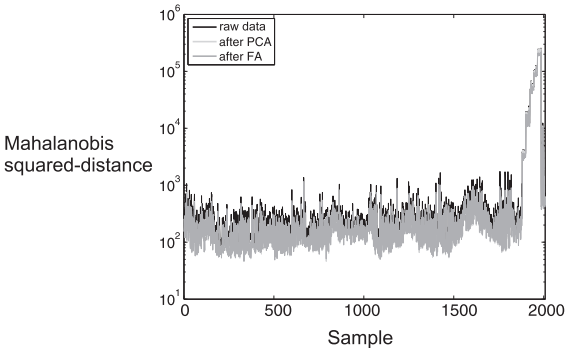

Fig. 9. Comparison of the Mahalanobis squared-distance applied to the raw feature vector with the Mahalanobis squared-distance computed after PCA and FA.

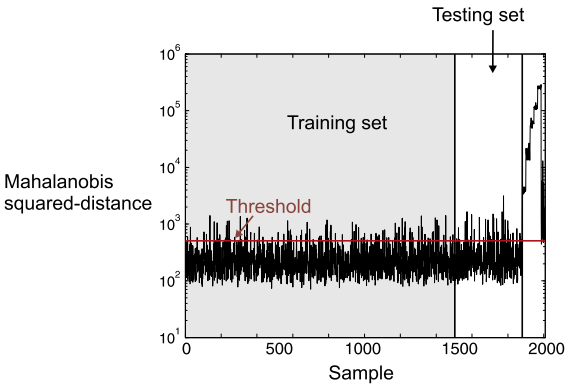

Fig. 10. Mahalanobis squared-distance and threshold for novelty detection using a normality assumption.

and selecting the model which gives the lowest error. The fitting of the parameters is performed using a differential evolution algorithm described in [35], and in the present case, the distribution giving the lowest error is the Frechet distribution:

$$H(x) = \begin{cases} \exp\left[-\left(\frac{\delta}{x-\lambda}\right)^{\beta}\right] & \text{if } x \geqslant 0 \\ 0 & \text{otherwise} \end{cases} \tag{40}$$

Once the parameters δ, λ and β are known, the threshold is computed for a confidence level α (=0.001 in the present case) by inverting the expression:

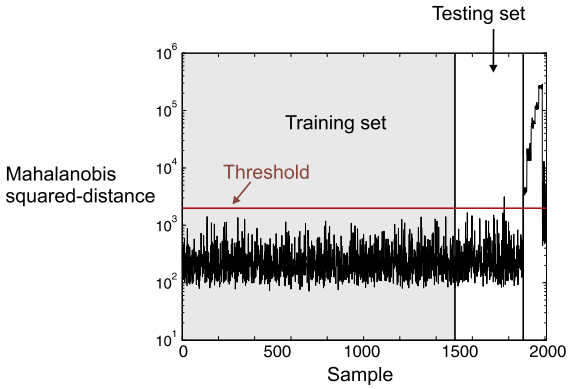

Fig. 11. Mahalanobis squared-distance and threshold for novelty detection using extreme value statistics – 80% of healthy condition used as training set.

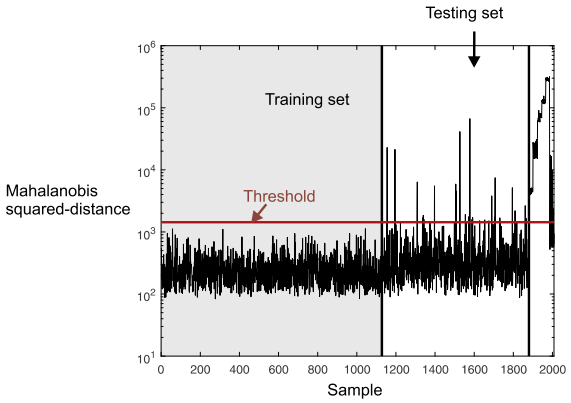

Fig. 12. Mahalanobis squared-distance and threshold for novelty detection using extreme value statistics – 60% of healthy condition used as training set.

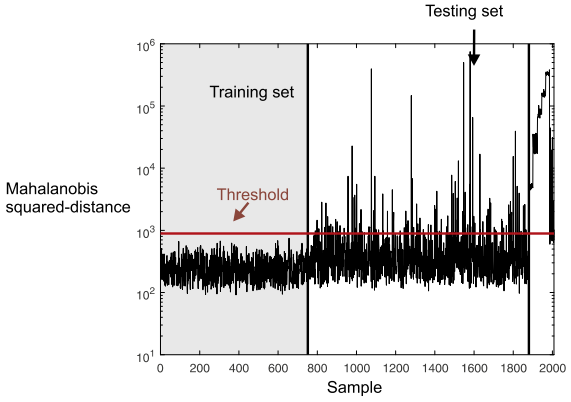

Fig. 13. Mahalanobis squared-distance and threshold for novelty detection using extreme value statistics – 40% of healthy condition used as training set.

$$\exp\left[-\left(\frac{\delta}{x-\lambda}\right)^{\beta}\right] = 1-\alpha/2 \tag{41}$$

which gives the threshold T_{EVS}:

$$T_{EVS} = x = \lambda + \frac{\delta}{(-ln(1-\alpha/2))^{1/\beta}} \tag{42}$$

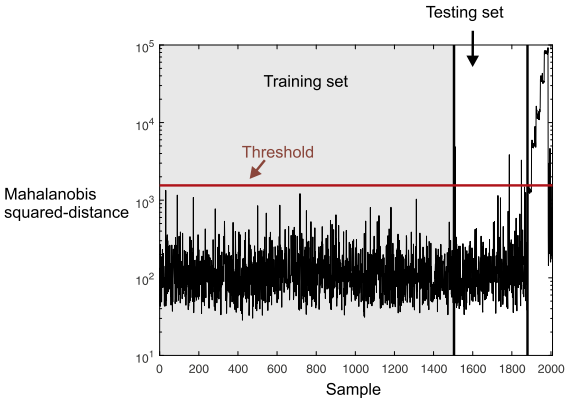

Fig. 14. Mahalanobis squared-distance and threshold for novelty detection using extreme value statistics – feature vector of size 135, 80% of healthy condition used as training set.

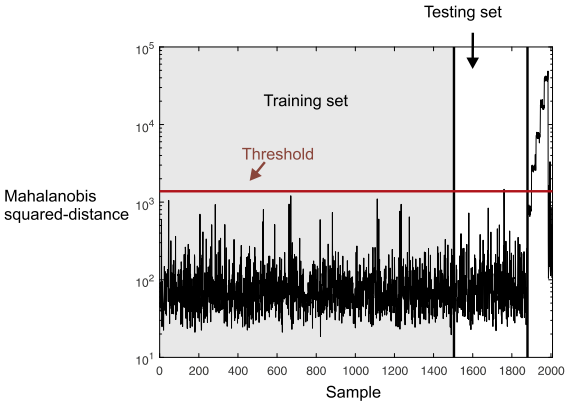

Fig. 15. Mahalanobis squared-distance and threshold for novelty detection using extreme value statistics – feature vector of size 90, 80% of healthy condition used as training set.

This threshold is represented in Fig. 11. The figure shows that this threshold is much more adequate than the one computed based on the normality assumption. There are no false positives in the training set and only one outlier in the testing set. All damaged samples lie above the threshold, showing that this type of threshold is adequate to perform damage detection under changing environmental conditions. Note however that after removing the point masses, the Mahalanobis squared-distance returns close to the original level but slightly above the threshold, at a level corresponding to the first level of damage. This is probably due to the fact that the training data did not include the full range of environmental conditions.

Figs. 12 and 13 show the influence of taking randomly respectively 60 and 40% of the healthy state in the training set instead of 80%. One sees clearly that the number of false positives in the testing set strongly increases and exceeds the confidence level of the threshold, showing that there are not enough samples in the training set. In the present case, at least 60–80% of the healthy state should be considered in the training data.

Figs. 14 and 15 show the influence of the size of the feature vector. In the first graph, only the real part of the mode shapes is considered and the imaginary part is discarded, resulting in a feature vector of size 135. In the second graph, the imaginary part and the high frequency modes (14–16) are discarded resulting in a feature vector of size 90. In both cases, the number of false positives is not strongly affected for the testing set, but the first damage scenario now lies below the computed threshold. This illustrates the fact that, as expected, by reducing the size of the feature vector, some information is lost and it is more difficult to differentiate the damage from the environmental conditions.

5. Conclusions

The Mahalanobis squared-distance is often used to perform novelty detection. By performing an eigenvalue decomposition of the covariance matrix used to compute that distance, it has been shown that the Mahalanobis squared-distance can be written as the sum of independent terms which result from a transformation from the feature vector space to a space of independent variables. In general, especially when the dimension of the feature vector is large, there are dominant eigenval-

ues and eigenvectors associated to the covariance matrix, so that a set of principal components can be defined. Because the associated eigenvalues are high, their contribution to the Mahalanobis squared-distance is low, while the contribution of the other components is high due to the low value of the associated eigenvalues. This analysis shows that the Mahalanobis squared-distance naturally filters out the variability in the training data. This property can be used to remove the effect of the environment in damage detection. It has also been shown that this method is closely related to the two main linear techniques used to remove confounding effects: principal component analysis and factor analysis. This has been demonstrated on real data from a wooden bridge for which the feature vector consists in eigenfrequencies and modeshapes collected under changing environmental conditions, as well as damaged conditions simulated with an added mass. The results confirm the ability to filter out environmental effects while keeping a high sensitivity to structural changes, and the equivalent performances of the new methodology proposed and the two established techniques. When filtering environmental effects, one should pay attention to using a proper training set containing the full range of environmental conditions, and to using a large enough feature vector in order to ensure some separability between the damage effects and the environmental effects. The results also show that the normality assumption does not hold in the case studied, and that an approach based on extreme value statistics is necessary to set a proper threshold for damage detection.

Acknowledgements

The authors wish to thank their friend and colleague Jyrki Kullaa from AALTO University in Finland for kindly providing the data from the wooden bridge. KW also gratefully acknowledges the support of the UK Engineering and Physical Sciences Research Council (EPSRC) through grant reference numbers EP/J016942/1 and EP/K003836/2.

References

[1] C.F. Farrar, K. Worden, Structural Health Monitoring: A Machine Learning Perspective, John Wiley & Sons, 2013.
[2] K. Worden, G. Manson, D. Allman, Experimental validation of a structural health monitoring methodology: Part I. Novelty detection on a laboratory structure, J. Sound Vib. 259 (2) (2003) 323–343.
[3] A. Deraemaeker, E. Reynders, G. De Roeck, J. Kullaa, Vibration-based structural health monitoring using output-only measurements under changing environment, Mech. Syst. Sign. Process. 22 (2008) 34–56.
[4] E. Reynders, Fully automated (operational) modal analysis, Mech. Syst. Sign. Process. 29 (2012) 228–250.
[5] M. Basseville, M. Abdelghani, A. Benveniste, Subspace-based fault detection algorithms for vibration monitoring, Automatica 36 (2000) 101–109.
[6] J. Kullaa, Damage detection of the Z24 bridge using control charts, Mech. Syst. Sign. Process. 17 (1) (2003) 163–170.
[7] K. Worden, G. Manson, N.R.J. Fieller, Damage detection using outlier analysis, J. Sound Vib. 229 (3) (2000) 647–667.
[8] H. Sohn, M. Dzwonczyk, E.G. Straser, K.H. Law, T. Meng, A.S. Kiremidjian. Adaptive modeling of environmental effects in modal parameters for damage detection in civil structures, in: Proceedings of SPIE, vol. 3325, 1998, pp. 127–138.
[9] B. Peeters, J. Maeck, G. De Roeck, Vibration-based damage detection in civil engineering: excitation sources and temperature effects, Smart Mater. Struct. 10 (2001) 518–527.
[10] B. Peeters, G. De Roeck, One-year monitoring of the Z24-bridge: environmental effects versus damage events, Earthq. Eng. Struct. Dynam. 30 (2001) 149–171.
[11] S. Alampalli, Effects of testing, analysis, damage and environment on modal parameters, Mech. Syst. Sign. Process. 14 (1) (2000) 63–74.
[12] A.M. Yan, G. Kerschen, P. De Boe, J.C. Golinval, Structural damage diagnosis under varying environmental conditions Part II: Local PCA for non-linear cases, Mech. Syst. Sign. Process. 19 (4) (2005) 865–880.
[13] V. Lämsä, J. Kullaa, Dynamical extension of nonlinear factor analysis in structural health monitoring to remove environmental effects, in: Proceedings of III ECCOMAS Thematic Conference on Smart Structures and Materials, Gdansk, Poland, July 2007.
[14] H. Sohn, K. Worden, C.R. Farrar, Novelty detection using auto-associative neural network, in: Proc 2001 ASME Int. Mech Eng. Congress and Exposition, New York, USA, November 2001.
[15] A.M. Yan, G. Kerschen, P. De Boe, J.C. Golinval, Structural damaged diagnosis under varying environmental conditions – Part I: A linear analysis, Mech. Syst. Sign. Process. 19 (4) (2005) 847–864.
[16] J. Kullaa, Structural health monitoring under variable environmental or operational conditions, in: Proc. of the second European Workshop on Structural Health Monitoring, Munich, Germany, 2004, pp. 1262–1269.
[17] R. De Maesschalck, D. Jouan-Rimbaud, D.L. Massart, The mahalanobis distance, Chemometr. Intell. Lab. Syst. 50 (2000) 1–18.
[18] H. Cao, X. Chen, Y. Zi, F. Ding, H. Chen, J. Tan, Z. He, End milling tool breakage detection using lifting scheme and mahalanobis distance, Mach. Tools Manuf. 48 (2008) 141–151.
[19] S.M. Ji, L.B. Zhang, J.L. Yuan, Y.H. Wan abd, X. Zhang, L. Zhang, G.J. Bao, Method of monitoring wearing and breakage states of cutting tools based on mahalanobis distance features, J. Mater. Process. Technol. 129 (2002) 114–117.
[20] W.C. Lai, T.P. Chang, J.J. Wang, C.W. Kan, W.W. Chen, An evaluation of mahalanobis distance and grey relational analysis for crack pattern in concrete structures, Comput. Mater. Sci. 65 (2012) 115–121.
[21] S. Park, D.J. Inman, C.B. Yun, An outlier analysis of MFC-based impedance sensing data for wireless structural health monitoring of railroad tracks, Eng. Struct. 30 (2008) 2792–2799.
[22] P.C. Wang, C.T. Su, K.H. Chen, N.H. Chen, The application of rough set and mahalanobis distance to enhance the quality of OSA diagnosis, Expert Syst. Appl. 38 (2011) 7828–7836.
[23] G. Taguchi, R. Jugulum, The Mahalanobis-Taguchi Strategy: A Pattern Technology System, John Wiley & Sons, New York, 2002.
[24] X. Jin, T.W.S. Chow, Anomaly detection of cooling fan and fault classification of induction motor using Mahalanobis-Taguchi system, Expert Syst. Appl. 40 (2013) 5787–5795.
[25] E.A. Cudney, J. Hong, R. Jugulum, K. Paryani, K.M. Ragsdell, G. Taguchi, An evaluation of Mahalanobis-Taguchi system and neural network for multivariate pattern recognition, J. Ind. Syst. Eng. 1 (2) (2007) 139–150.
[26] E.A. Cudney, D. Drain, K. Paryani, N. Sharma, A comparison of the Mahalanobis-Taguchi system to a standard statistical method for defect detection, J. Ind. Syst. Eng. 2 (4) (2009) 250–258.
[27] C.W. Kim, R. Isemoto, K. Sugiura, M. Kawatani, Structural fault detection of bridges based on linear system parameter and MTS method, J. JSCE 1 (2013) 32–43.
[28] G. Manson, Identifying damage sensitive, environment insensitive features for damage detection, in: Proceedings of the Third International Conference on Identification in Engineering Systems, 2002.

[29] E. Cross, G. Manson, K. Worden, S.G. Pierce, Features for damage detection with insensitivity to environmental and operational variations, Proc. Roy. Soc. A (2012), https://doi.org/10.1098/rspa.2012.0031.
[30] S. Sharma, Applied Multivariate Techniques, John Wiley & Sons, New York, 1996.
[31] G. Tondreau, E. Reynders, A. Deraemaeker, Towards a more realistic modelling of the uncertainty on identified mode shapes due to measurement noise, in: Proc DAMAS 2011, Oxford, UK, July 2011.
[32] J. Kullaa, Structural health monitoring of a crane in variable configurations, in: Proceedings of ISMA 2004, Leuven, Belgium, 2004, pp. 457–469.
[33] J. Kullaa, Eliminating environmental or operational influences in structural health monitoring using the missing data analysis, J. Intell. Mater. Syst. Struct. 20 (2009) 1381–1390.
[34] K. Worden, D.W. Allen, H. Sohn, D.W. Stinemates, C.R. Farrar, Extreme Value Statistics for Damage Detection in Mechanical Structures, Los Alamos Technical Report LA-13903-MS, 2002.
[35] K. Worden, G. Manson, H. Sohn, C.R. Farrar, Extreme value statistics from differential evolution for damage detection, in: Proc IMAC XXIII, Orlando, USA, February 2005.
[36] E. Castillo, Extreme Value Theory in Engineering, Academic Press Series in Statistical Modeling and Decision Science, San Diego, CA, 1988.